# International Conference on Space Optics—ICSO 2022

Dubrovnik, Croatia

3–7 October 2022

*Edited by Kyriaki Minoglou, Nikos Karafolas, and Bruno Cugny,*

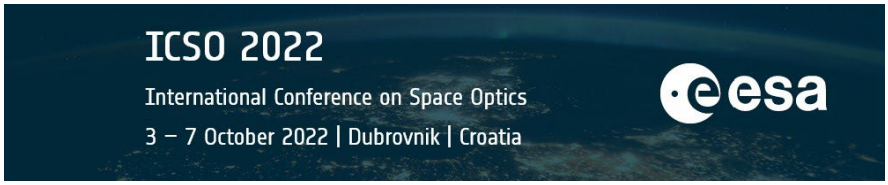


# *Preliminary DIMM-Based Analysis of Atmospheric Turbulence by Using Optical Data Relay Satellite "LUCAS"*


International Conference on Space Optics — ICSO 2022, edited by Kyriaki Minoglou, Nikos Karafolas, Bruno Cugny, Proc. of SPIE Vol. 12777, 127775L · © 2023 ESA and CNES · 0277-786X · doi: 10.1117/12.2691031

# Preliminary DIMM-Based Analysis of Atmospheric Turbulence by Using Optical Data Relay Satellite "LUCAS"

Yuma Abe[a], Hideaki Kotake[a], Yoshihiko Saito[a], Dimitar R. Kolev[a], Yasuhiro Takahashi[a], Takuya Okura[a], Tetsuharu Fuse[a], Yohei Satoh[b], Takamasa Itahashi[b], Shiro Yamakawa[b], and Morio Toyoshima[a]

[a]National Institute of Information and Communications Technology (NICT), 4–2–1 Nukui-kitamachi, Koganei, Tokyo, 184–8795 Japan
[b]Japan Aerospace Exploration Agency (JAXA), 2–1–1 Sengen, Tsukuba, Ibaraki, 223–8522 Japan

## ABSTRACT

This paper presents analytical results of atmospheric turbulence for optical communication links between a geostationary earth orbit (GEO) satellite and an optical ground station (OGS) by using a differential image motion monitor (DIMM) method. Optical satellite communications are expected to increase the transmission capacity of satellite-ground communication links. However, atmospheric turbulence degrades the communication performance of satellite-ground optical links. In order to practically utilize satellite-ground optical links, measurement data of atmospheric turbulence are helpful for the optical system design for OGSs. Therefore, we have conducted satellite-ground optical link experiments between the Laser Utilizing Communication System (LUCAS) onboard the optical data relay GEO satellite and an OGS in Okinawa. In this paper, we report preliminary analytical results of the Fried parameter measured by using the DIMM method and provide statistical results of the parameter.

**Keywords:** Optical Satellite Communications, Atmospheric Turbulence, Differential Image Motion Monitor (DIMM)

## 1. INTRODUCTION

Various optical satellite link experiments have been conducted since the world's first success for a trial of satellite-ground communications by the Engineering Test Satellite-VI (ETS-VI) in 1994.[1] Optical satellite communication has been attracting much attention as one of the new enablers of communication between satellites and the ground because it enables higher-capacity communication, lighter weight of communication terminals, and lower power consumption than radio frequency communication. However, atmospheric turbulence strongly interrupts the communication performance of satellite-ground optical links. Therefore, it is necessary to investigate the atmospheric turbulence loss for the optical system design of satellite-ground optical communication. In addition, adaptive optics is one of the key solutions to compensate for atmospheric turbulence. Therefore, atmospheric turbulence data is also utilized to design adaptive optics for optical ground stations (OGSs).

Measurement of atmospheric turbulence has been actively conducted mainly in the field of astronomy. The well-known atmospheric turbulence parameters are the scintillation index $\sigma_I$, the atmospheric refractive-index structure parameter $C_n^2$, and the Fried parameter $r_0$.[2] The scintillation index represents the normalized variation of the signal, the atmospheric structure parameter represents the intensity of atmospheric turbulence, and the Fried parameter defines the maximum spatial scale at which the wavefront is considered to be maintained.[3] In the field of optical satellite communications, atmospheric structure parameters and Fried parameters have been calculated through optical communication experiments using satellites. For example, $r_0$ is calculated as 4.2 cm and 4.7 cm at a wavelength of 847 nm in the experiment using the Optical Inter-orbit Communications Engineering Test Satellite (OICETS),[4] and $r_0$ is calculated as 10-25 cm at a wavelength of 1550 nm in the

Further author information: (Send correspondence to Yuma Abe)
Yuma Abe: E-mail: yuma.abe@nict.go.jp

experiment using the Small Optical TrAnsponder (SOTA).[5] However, the atmospheric turbulence parameters obtained by optical communication experiments have not been fully reported because the atmospheric turbulence varies with region, environment, and wavelength.

The authors have been jointly conducting experiments and operations of optical satellite communications between a geostationary earth orbit (GEO) satellite and an OGS since 2021 to evaluate atmospheric propagation and communication characteristics for the practical application of satellite-ground optical communications. In these experiments and operations, we utilize the Laser Utilizing Communication System (LUCAS) onboard the optical data relay GEO satellite developed by the Japan Aerospace Exploration Agency (JAXA). The LUCAS implements a laser in the 1550nm band.[6] Moreover, we utilize an OGS with a 1-meter telescope installed at the Okinawa Electromagnetic Technology Center of the National Institute of Information and Communications Technology (NICT).

In this paper, we present the initial analytical results of the Fried parameter, one of the atmospheric turbulence parameters, calculated using the differential image motion monitor (DIMM) method for the optical communication experiment conducted in November 2021. Furthermore, we compare the Fried parameter with the scintillation index measured in this experiment.

## 2. ATMOSPHERIC TURBULENCE AND DIMM METHOD

This section provides an overview of two atmospheric turbulence parameters; the refractive-index structure parameter and the Fried parameter, and an overview of the DIMM method to derive the Fried parameter from the optical satellite communication experiment.

### 2.1 Refractive-index structure parameter and Fried parameter

Atmospheric turbulence is a refractive index fluctuation caused by atmospheric density and temperature fluctuation. The atmosphere is discretely distributed up to an altitude of approximately 20 km, and atmospheric turbulence intensity is known to increase as closer to the earth's surface.[2] It has also been reported that several atmospheric turbulence layers with different strengths.

Let $n(x)$ be an atmospheric refractive index of the atmosphere at position $x$. According to Kolmogorov's theory, a structure function of the atmospheric refractive index is represented by

$$D_n(r) = \langle (n(x) - n(x+r))^2 \rangle = C_n^2 r^{2/3}. \tag{1}$$

Here, for a given physical quantity, the structure function is defined as the average of the squares of the differences of the values at locations separated by a certain distance $r$. The parameter $C_n^2$ in Eq. (1) is called the *refractive-index structure parameter* and represents the strength of the atmospheric turbulence. Let $C_n^2(h)$ be a refractive-index structure function of a height $h$. One of the widely known mathematical models for the refractive-index structure parameter is the Hufnagel-Valley (H-V) model,[7] which is defined as

$$C_n^2(h) = 0.00594(w/27)^2(10^{-5}h)^{10}\exp(-h/1000) + 2.7\times 10^{-16}\exp(-h/1500) + A\exp(-h/100), \tag{2}$$

where $A = C_n^2(0)$ is a ground-level value of $C_n^2$ and $w$ is a root-mean-square windspeed (called pseudo-wind). The root-mean-square windspeed is modeled by

$$w = \left[\frac{1}{15\times 10^3}\int_{5\times 10^3}^{20\times 10^3} V^2(h)\mathrm{d}h\right]^{1/2},$$

$$V(h) = \omega_s h + V_g + 30\exp\left[-\left(\frac{h-9400}{4800}\right)^2\right],$$

where $\omega_s$ is the slew rate associated with a satellite moving with respect to the ground and $V_g$ is the ground wind speed.

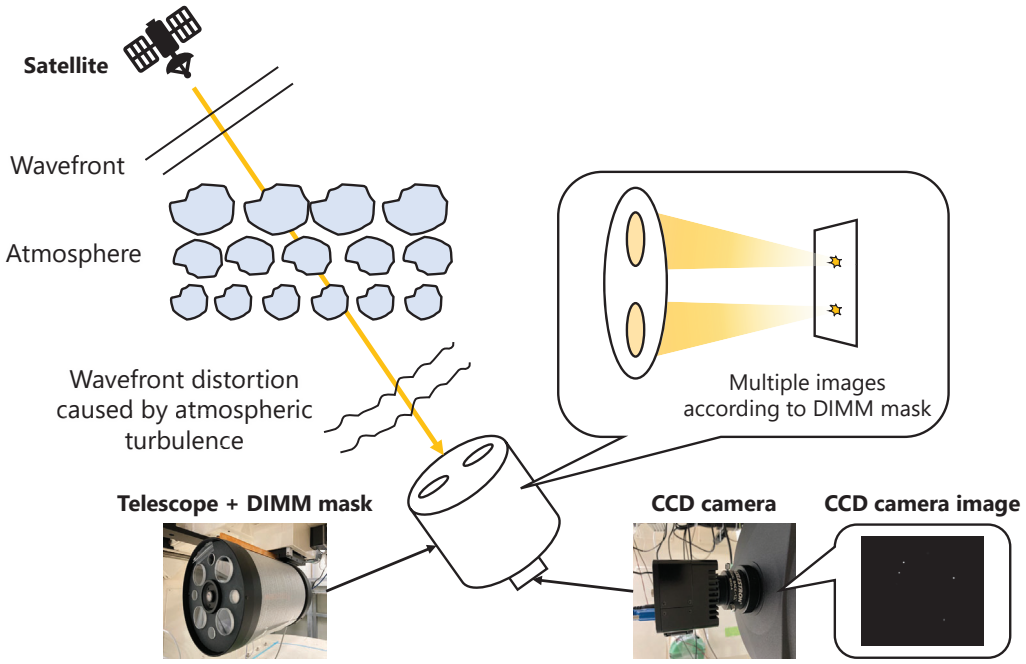


Figure 1: The DIMM system covered in this paper.

The Fried parameter $r_0$ can be calculated by

$$r_0 = \left( \frac{0.423k^2}{\cos\zeta} \int_0^L C_n^2(h)\mathrm{d}h \right)^{-3/5}, \tag{3}$$

where $k = 2\pi/\lambda$, $\lambda$, and $\zeta$ denote the wavenumber, wavelength, and zenith angle, respectively, and $\int_0^L$ represents an integral along the optical path from the light source to the telescope.[7] Therefore, the Fried parameter is defined as the value obtained by integrating the refractive-index structure function along the optical path. Note that the smaller this value is, the greater the atmospheric turbulence. Furthermore, the Fried parameter $r_0$ is proportional to $\lambda^{6/5}$ from Eq. (3).

## 2.2 DIMM METHOD

The DIMM method is one of the methods to directly derive the Fried parameter from positional fluctuations of images.[8,9]

Figure 1 shows the DIMM measurement system we focus on in this paper. In the DIMM measurement system, a mask with multiple apertures (hereafter, DIMM mask) is implemented on the front of the telescope, and a charge coupled device (CCD) camera is also implemented on the back of the telescope. A schematic diagram of the DIMM mask attached in front of the telescope is shown in Fig. 2. The symbols $D$ and $d$ represent aperture diameter and distance between the two apertures, respectively. The direction parallel to the two apertures is called the longitudinal direction, and the direction perpendicular to the longitudinal direction is called the transversal direction. A prism is attached to each aperture of the DIMM mask, and its angle is adjusted so that multiple images corresponding to each aperture are obtained on the CCD camera. The images captured by the CCD camera move differently because the optical signal passing through the different apertures is affected by the atmospheric turbulence while propagating through different paths. The atmospheric turbulence is then obtained by analyzing the relative positions of these multiple images.

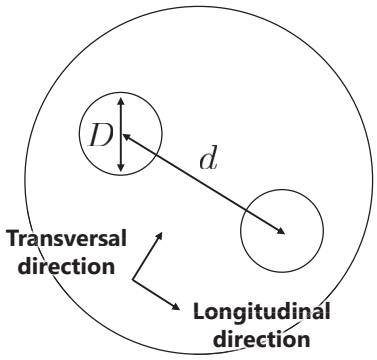


Figure 2: The diagram of the DIMM mask.

The Fried parameters in the longitudinal and transversal directions are calculated by

$$r_{0,l} = \left\{ \frac{2\lambda^2}{\sigma_l^2} \left( 0.179 D^{-1/3} - 0.0968 d^{-1/3} \right) \right\}^{3/5}, \tag{4}$$

$$r_{0,t} = \left\{ \frac{2\lambda^2}{\sigma_t^2} \left( 0.179 D^{-1/3} - 0.145 d^{-1/3} \right) \right\}^{3/5}, \tag{5}$$

respectively.[8,9] The symbols $\sigma_l^2$ and $\sigma_t^2$ represent the variance of the angular distance of the longitudinal and transversal directions, respectively, and these can be calculated by the relative position of the images obtained by the CCD camera. Finally, we obtain the total Fried parameter by using the Fried parameters both in the longitudinal and transversal directions as

$$r_0 = \sqrt{r_{0,l}^2 + r_{0,t}^2}. \tag{6}$$

The procedure for the DIMM-based calculation of the Fried parameter is shown below.

**Procedure 1.** The procedure for the DIMM-based calculation of the Fried parameter:

Step 1: Capture the images in RGB color obtained from the CCD camera and apply grayscaling and binarization to the images*.

Step 2: Calculate the center-of-gravity position of each image in each frame and the average of the center-of-gravity positions of all frames.

Step 3: Using the average of the center-of-gravity positions obtained in Step 2, transform the center-of-gravity positions of the two images from the CCD camera coordinate system to that in the longitudinal and transversal directions in all frames.

Step 4: Cut out frames for each analysis interval defined by the user.

Step 5: In each frame, calculate the Euclidean distance and angular distance of the center-of-gravity of two images in each direction.

Step 6: Calculate the variance of the angular distance of the center-of-gravity of the two points in each direction through the analysis interval.

Step 7: Calculate the Fried parameters $r_{0,l}$ and $r_{0,t}$ by using Eqs. (4)-(5) and the total Fried parameter $r_0$ by using Eq. (6).

Step 8: Repeat from Step 4 to Step 7 for each analysis interval.

*We need some preprocessing, e.g., exclusion of saturated frames in the grayscale image and exclusion of frames whose number of pixels is less than the predetermined threshold value in the binarized image.

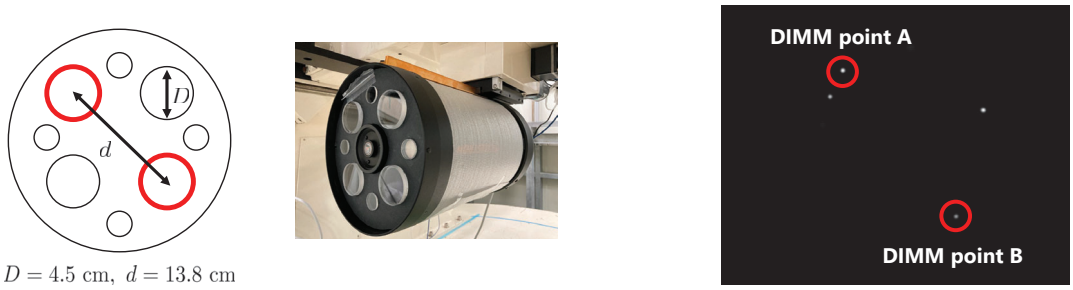


(a) (b)

Figure 3: (a) A DIMM mask used in this experiment. (b) Image obtained with CCD camera and two selected points used for analysis.

Table 1: Parameters in our experiments.

| Parameter | Value | Unit |
|---|---|---|
| DIMM telescope | | |
| Aperture diameter | 203 | mm |
| Focal length | 1260 | mm |
| CCD camera | | |
| Pixel size | 20 x 20 | $\mu$m |
| Pixel number | 320 x 256 | pixels |
| Pixel array | 6.4 x 5.12 | mm |
| Frame rate | 40 | fps |
| DIMM mask (Fig. 3a) | | |
| Aperture diameter $D$ | 4.5 | cm |
| Distance between two apertures $d$ | 13.8 | cm |

## 3. EXPERIMENT SETUP

At the OGS of the Okinawa Electromagnetic Technology Center of NICT, we installed a telescope with a 1-meter aperture (hereafter, 1-meter telescope). In addition, we also implemented a telescope with a 203 mm aperture (hereafter, DIMM telescope) on the bottom of the 1-meter telescope. We utilized the 1-meter telescope for the optical satellite link experiment with the LUCAS[10] and the DIMM telescope for calculating the Fried parameter using the DIMM method. Here, the optical signal emitted from the LUCAS is propagated through a satellite-ground optical path and received by the OGS. Therefore, after the 1-meter telescope tracks the LUCAS, the DIMM telescope can also capture the images of the optical signal using the CCD camera.

The DIMM mask used in this experiment is shown in Fig. 3a, and an example of images obtained by the CCD camera is shown in Fig. 3b. The DIMM mask in Fig. 3a has four apertures of two types, one large and one small, with different aperture diameters. In this paper, we applied the DIMM method to the red-circled two images shown in Fig. 3b, which corresponded to the two red-circled apertures in Figure 3a. The parameters of this experimental setup are also shown in Table 1.

## 4. EXPERIMENT RESULTS AND ANALYSIS

In this section, we present the results of the Fried parameter obtained through our experiments and analysis.

Fried parameters were calculated by analyzing 30 successful acquisition and tracking paths in the optical communication experiment between the LUCAS and the OGS conducted in November 2021. We set the data acquisition time for each experimental path to 60 s and the analysis interval indicated in Step 4 of Procedure 1 to 1 s. Therefore, the Fried parameter was obtained every 1 s in each experimental path.

Table 2: Experiment paths that is shown in Fig. 4. Time is represented by Japan Standard Time (JST).

| Path ID | Date (JST) | Time | Mean of Fried parameter | Mean of scintillation index |
|---|---|---|---|---|
| A | 2022/11/11 | 00:49:20 - 00:50:20 | 24.5 cm | 0.22 |
| B | 2022/11/12 | 03:13:00 - 03:14:00 | 17.9 cm | 0.33 |
| C | 2022/11/15 | 04:04:50 - 04:05:50 | 14.8 cm | 0.20 |
| D | 2022/11/19 | 01:53:00 - 01:54:00 | 13.9 cm | 0.33 |

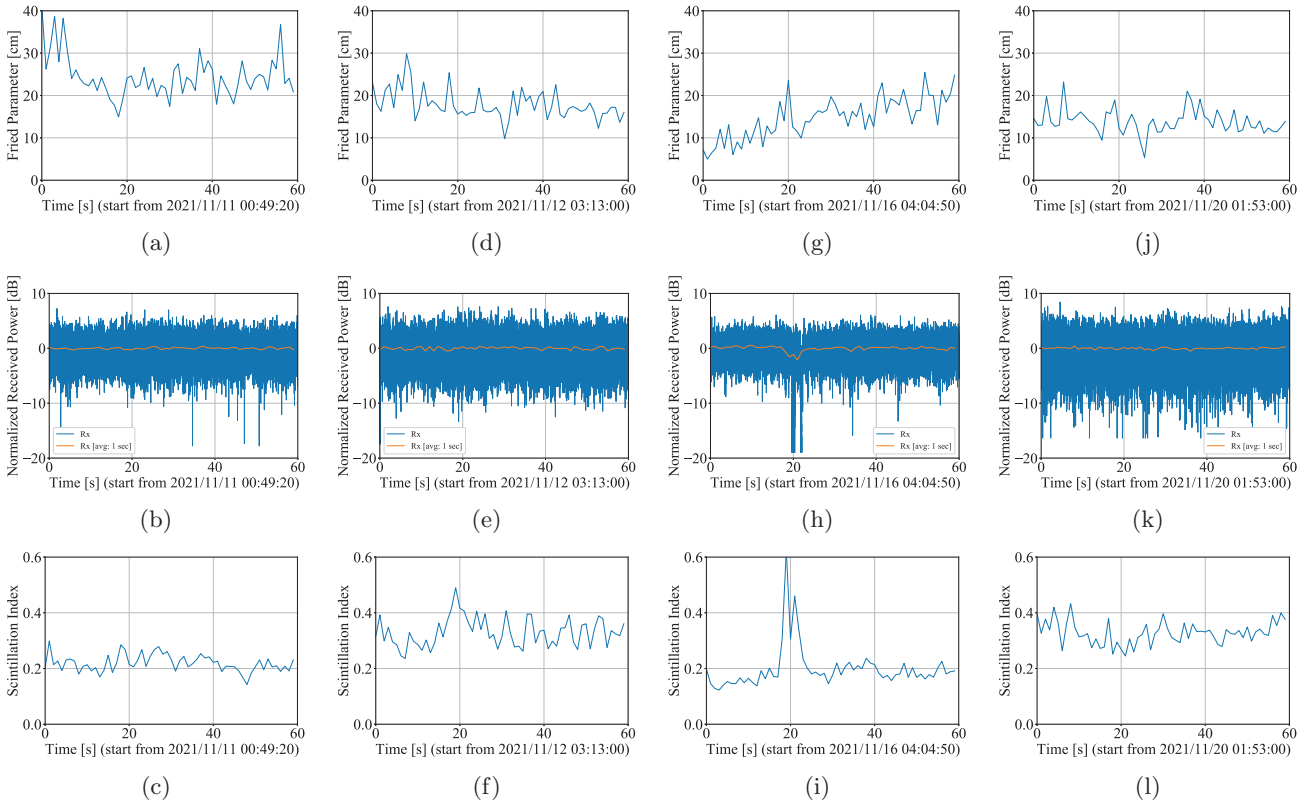


Figure 4: The experiment results in the four experimental paths; A (a–c), B (d–f), C (g–i), and D (j–l) shown in Table 2. (a, d, g, j) Time series of the Fried parameter. (b, e, h, k) Time series of the normalized received power. (c, f, i, l) Time series of the scintillation index.

As an example, Fig. 4 shows the time variability of the Fried parameters of four experimental paths shown in Table 2. For reference, we also show the received power measured by the photodetector placed on the side of the 1-meter telescope, and the scintillation index was calculated from the received power. The sampling frequency of the received power is set as a few kHz, and it is normalized by the average value of the whole interval. The scintillation index $\sigma_I$ is given by

$$\sigma_I = \frac{\langle I_k^2 \rangle - \langle I_k \rangle^2}{\langle I_k \rangle^2} = \frac{\langle I_k^2 \rangle}{\langle I_k \rangle^2} - 1, \tag{7}$$

where $I_k$ is the time series of received power and $\langle A \rangle$ is the operator that calculates the expected value of the physical quantity $A$. The scintillation index is the normalized variation value of the signal. This parameter indicates that $\sigma_I = 0$ when there is no variation and $\sigma_I > 1$ when there is a significant variation. Figures 4c, 4f, 4i, and 4l represent the scintillation index computed for the interval 1 s. The mean Fried parameters for 60 s in the four experimental paths were 24.5 cm, 17.9 cm, 14.8 cm, and 13.9 cm, respectively, and the scintillation index averaged 0.22, 0.33, 0.20, and 0.33, respectively. Smaller Fried parameters and larger scintillation indices mean

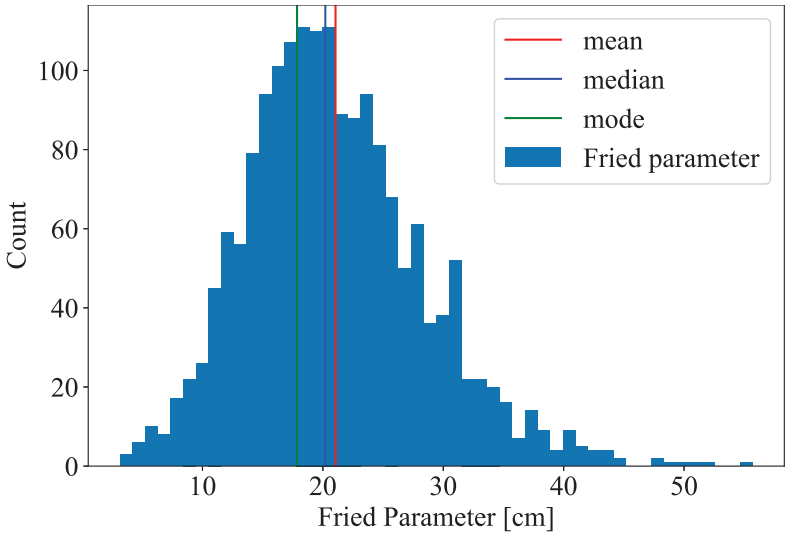


Figure 5: Histogram of Fried parameters obtained in the experiment (1767 samples in the 30 experimental paths).

more considerable atmospheric turbulence and signal variations. From these results, the relationship between the Fried parameter and scintillation index was in line with the theory for the former two experimental paths, A and B. However, the relationship did not always hold compared to other experimental path combinations. Especially, the time interval when $\sigma_I$ in Fig. 4i rapidly increased, $r_0$ in Fig. 4g did not increase in the experimental path C.

A histogram of all Fried parameters obtained in this experiment is shown in Fig. 5. The Fried parameters were obtained for 1770 samples in all 30 experimental paths because we set the data acquisition time to 60 s and the analysis interval to 1 s. However, as indicated in Section 2, some frames were excluded from the analysis due to the cloud and weather conditions. Therefore, the final sample size was 1767. Note that these samples include several cases where the acquisition and tracking were successful but under bad conditions. The mean, median, and mode of the Fried parameters were 21.1 cm, 20.2 cm, and 17.9 cm, respectively. When we used the H-V model of the refractive-index structure parameter in Eq. 2 and the Fried parameter in Eq. 3, the Fried parameter was calculated to be 15.7 cm. The parameters in these equations were set to $\omega_s = 0, V_g = 0, A = C_n^2(0) = 1.7 \times 10^{-14}$, and $L = 36,000 \times 10^3$. Finally, we compare the results with other experiments described in Section 1. As for the OICETS, the Fried parameter was 4.2 cm and 4.7 cm, which was smaller than the Fried parameter obtained in this experiment. The wavelength used in the OICES was 847 nm, and this experiment used 1550 nm. The Fried parameter depends on the wavelength and is proportional to $\lambda^{6/5}$; thus, we confirmed the relationship was consistent with the theory. Furthermore, the statistical values of the Fried parameter obtained in this experiment were within the range of the Fried parameters obtained by the SOTA, which used the same wavelength of 1550 nm as this experiment. These results showed that the parameters calculated using the DIMM method are reasonable. Therefore, we concluded we derived the statistical values of the Fried parameters between the LUCAS and the OGS at Okinawa.

## 5. CONCLUSION

This paper presented the analytical results of the Fried parameters using the DIMM method for the optical link experiment conducted in November 2021 between the LUCAS on board the GEO satellite and the OGS at NICT Okinawa, Japan. We calculated the mean, median, and mode of the Fried parameters between the LUCAS and the OGS and found they were 21.1 cm, 20.2 cm, and 17.9 cm, respectively. In future works, we will analyze the relationship between Fried parameters and scintillation index and the reliability of Fried parameters. Furthermore, we plan to conduct optical communication experiments regularly to analyze the seasonal and weather dependence of the Fried parameter.

## ACKNOWLEDGEMENT

The authors acknowledge NEC Corporation, Nishimura Co., Ltd., and Space Engineering Development Co., Ltd. for their supports in our experiments.

## REFERENCES

[1] Toyoshima, M., "Recent trends in space laser communications for small satellites and constellations," *Journal of Lightwave Technology* **39**(3), 693–699 (2021).

[2] Hardy, J. W., [*Adaptive Optics for Astronomical Telescopes*], Oxford University Press (1998).

[3] Fried, D., "Statistics of a geometric representation of wavefront distortion," *Journal of Optical Society of America* **55**(11), 1427–1435 (1965).

[4] Toyoshima, M., Takenaka, H., and Takayama, Y., "Atmospheric turbulence-induced fading channel model for space-to-ground laser communications links," *Optics Express* **19**(17), 15965–15975 (2011).

[5] Kolev, D. R. and Toyoshima, M., "Satellite-to-ground optical communications using small optical transponder (SOTA) - received-power fluctuations," *Optical Express* **25**(23), 28319–28329 (2017).

[6] Yamakawa, S., Satoh, Y., Itahashi, T., Takano, Y., Hoshi, S., Miyamoto, Y., Sugiho, M., Yoshizawa, T., Koizumi, Y., Yukizane, M., Suzuki, S., and Kohata, H., "LUCAS: The second-generation geo satellite-based space data-relay system using optical link," in [*Proceedings of the 2022 IEEE International Conference on Space Optical Systems and Applications (ICSOS)*], 14–16 (2022).

[7] Andrews, L. C. and Phillips, R. L., [*Laser Beam Propagation through Random Media*], SPIE, second edition ed. (2005).

[8] Sarazion, M. and Roddier, F., "The ESO differential image motion monitor," *Astronomy and Astrophysics* **227**(1), 294–300 (1990).

[9] Tokovinin, A., "From differential image motion to seeing," *Publications of the Astronomical Society of the Pacific* **114**(800), 1156–1166 (2002).

[10] Kotake, H., Abe, Y., Takahashi, Y., Okura, T., Fuse, T., Satoh, Y., Itahashi, T., Yamakawa, S., and Toyoshima, M., "First experimental demonstration of optical feeder link by using the optical data relay satellite "LUCAS"," in [*Proceedings of the 2022 International Conference on Space Optics (ICSO)*], (2022, to be published).